

Cross-seam Hybrid MTDC System for Integration and Delivery of Large-scale Renewable Energy

Kaiqi Sun, Huangqing Xiao, Jiuping Pan, and Yilu Liu

Abstract—To better utilize the diversity of renewable energies in the U.S., this paper proposes a cross-seam hybrid multi-terminal high-voltage direct current (MTDC) system for the integration of different types of renewable energies in the U.S. Based on a developed station-hybrid converter design, the proposed hybrid MTDC system further investigates the connection methods of renewable energies and develops novel flexible power flow control strategies for realizing uninterrupted integration of renewable energies. In addition, the frequency response control of the hybrid MTDC system is proposed by utilizing the coordination between the converters in the hybrid MTDC system. The feasibility of the hybrid MTDC system and the performance of its corresponding control strategies are conducted in the PSCAD/EMTDC simulation. The simulation results indicate that the proposed hybrid MTDC system could realize the uninterrupted integration of renewable energies and flexible power transmission to both coasts of U.S.

Index Terms—Multi-terminal high-voltage direct current (MTDC) system, cross-seam interconnections, integration of large-scale renewable energies, flexible power flow control, frequency response control.

I. INTRODUCTION

NORTH America features some of the world's richest hydro, wind, solar, and other types of renewable energy resources [1]. As the fastest-growing energy source in the U.S., renewable energy installation increased about 100% from 2000 to 2018 [2].

The location selection of renewable energy generation inevitably depends on the geographical distribution [3]. As shown in [4]–[5], the locations of the potentially highest wind generation areas and solar energy generation sites in the U.S. are not overlapping. In addition, the output of wind and solar power generation is random and discontinuous.

Manuscript received: January 11, 2021; accepted: June 10, 2021. Date of CrossCheck: June 10, 2021. Date of online publication: September 2, 2021.

This work made use of the Engineering Research Center Shared Facilities supported by the Engineering Research Center Program of the National Science Foundation and DOE under NSF award (No. EEC-1041877) and the CURENT Industry Partnership Program.

This article is distributed under the terms of the Creative Commons Attribution 4.0 International License (<http://creativecommons.org/licenses/by/4.0/>).

K. Sun and Y. Liu are with the University of Tennessee, Knoxville, TN 37996, USA, and Y. Liu is also with the Oak Ridge National Laboratory, Oak Ridge, TN 37831, USA (e-mail: ksun8@utk.edu; liu@utk.edu).

H. Xiao (corresponding author) is with the School of Electric Power Engineering, South China University of Technology, Guangzhou 510641, China (e-mail: xiaohq@scut.edu.cn).

J. Pan is with the Hitachi ABB Power Grids Research, Raleigh, NC 27606, USA (e-mail: jiuping.pan@hitachi-powergrids.com).

DOI: 10.35833/MPCE.2021.000008

The intermittent nature and resource-dependent characteristic of renewable energies bring strong uncertainty for the power system operation [6]. Moreover, the time zone difference in the U.S. further enlarges the diversity of renewable energy utilization from the east coast to the west coast. As the penetration of renewable energies increases, the local power grid cannot fully consume the renewable energies, the bulk power and long-distance transmission in the U.S. become the requirements for the integration of large-scale renewable energies to the remote load centers.

At present, the three interconnections of the U.S. power grid, i.e., the Western Interconnection (WI), the Eastern Interconnection (EI), and the Electric Reliability Council of Texas (ERCOT), are almost independently operated with others [7]. Between the two interconnections, only a few high-voltage direct current (HVDC) interties exist and the transferring power between the interconnections is little. The recent Department of Energy (DOE) study has identified options with HVDC transmission technologies for enhancing the U.S. power grid to become a more integrated system that could increase the utilization and penetration of the national abundant renewable energies [7]. The primary design is the development of multiple high-capacity cross-seam HVDC transmission systems. These HVDC systems could be developed as multi-terminal HVDC (MTDC) systems with intermediate terminals for the integration of large-scale wind or solar power plants, as shown in Fig. 1 [7].

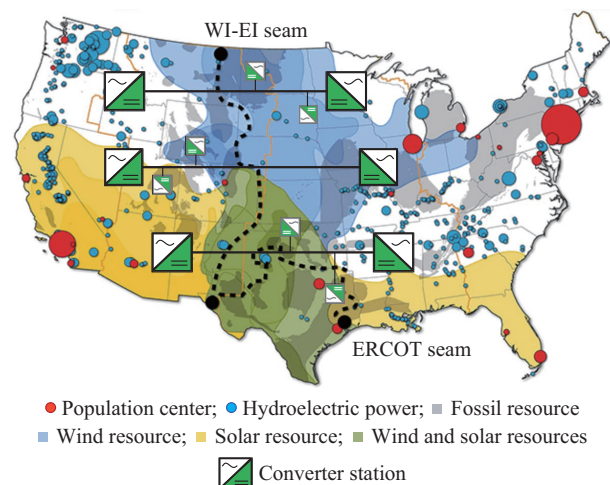


Fig. 1. Modified design based on Interconnection seam study.

For the cross-seam MTDC system shown in Fig. 1, the de-

sired solution needs to have the following combined features in order to realize the integration of large-scale renewable energies in the U.S.: ① high-capacity power transmission with magnitude of several GWs; ② operation flexibility with bidirectional power flow transmission.

In [7], the cross-seam HVDC lines have been designed with consideration of traditional line commutated converter based HVDC (LCC-HVDC) technology. LCC-HVDC is a mature technology for high-capacity power transmission with lower power losses and construction costs [8]. However, for power flow reversal as required by bidirectional power transmission of the cross-seam interconnections, the operation of LCC-HVDC system must be stopped temporarily to change the voltage polarity, which may also have negative impacts on the interconnected renewable power plants [9]. The voltage source converter based HVDC (VSC-HVDC) technology has achieved significant advancements during the last decade in terms of increased capacity ratings, reduced costs, and reduced losses [10], [11]. However, the cost of the VSC-HVDC system is still relatively higher [12] than that of LCC-HVDC for the GW-level transmission systems.

Combining the LCC and VSC technologies, the hybrid HVDC system is an attractive solution to the aforementioned trade-off [12]-[14]. In general, there are three types of hybrid HVDC systems in operation or under investigation: ① pole-hybrid system (the HVDC system where LCC and VSC are configured in different poles); ② terminal-hybrid system (the HVDC system where LCC and VSC are configured in different terminals); ③ converter-hybrid system (the HVDC system where LCC and VSC are formed by one converter) [15]-[18]. The pole-hybrid system is only applicable to the bipolar system and cannot be used in a monopolar system. It is difficult for the converter-hybrid systems to realize the power flow reversal because the DC current flowing through the LCC cannot be changed. The terminal-hybrid HVDC systems are designed mainly for unidirectional power transmission and not suitable for cross-seam interconnections. Thus, the existing hybrid HVDC solutions are not recommended for solving the current bulk power transmission issues in the U.S. power grid. In order to satisfy the requirement of cross-seam interconnection in the U.S. power grid, a station-hybrid HVDC scheme is proposed in our previous research [19]. The proposed structure could enable the flexible power

flow reversal, thereby realizing uninterrupted bidirectional power flows. However, this hybrid scheme is a two-terminal HVDC system scheme, with which the integration of renewable energies cannot be achieved.

Based on the station-hybrid converter (SHC) proposed in [19], this paper develops a hybrid MTDC system for the integration of large-scale renewable energies. Different from [19], the proposed hybrid MTDC system focuses on the coordination of the SHCs and renewable energy connecting (REC) converters, thereby achieving the uninterrupted integration of renewable energies and transmitting electric power to most of the U.S. The main contributions of this paper could be summarized as follows.

- 1) A novel topology of the hybrid MTDC system is proposed for cross-seam bulk power transmission and integration of large-scale renewable energies.
- 2) The basic operation control of the hybrid MTDC system and the connection configurations of the renewable energies into a hybrid MTDC system are analyzed.
- 3) The flexibility of power flow control strategies of the proposed hybrid MTDC system is investigated for realizing the uninterrupted integration of renewable energies.
- 4) The frequency response control (FRC) strategies of the proposed hybrid MTDC system are explored for improving the frequency stability of the interconnected power systems.

II. TOPOLOGY AND CONTROL STRUCTURE OF PROPOSED HYBRID MTDC SYSTEM

A. Structure of Hybrid MTDC System

Figure 2 depicts the structure of the hybrid MTDC system, which is composed of two SHCs and several intermediate REC converters. Each SHC is composed of one LCC and one VSC. The two different SHCs are connected to the same DC line, which saves the transmission corridor. On the DC side of each LCC, a reversal switch (RS) mechanism is configured for realizing the power flow reversal. Considering the operation stability and controllability, VSC technology is a practical solution for the requirements of the integration of renewable energies in the U.S. power grid [20]-[22]. In this hybrid MTDC system, the half-bridge (HB) VSC is adopted as the REC converter in the proposed hybrid MTDC system.

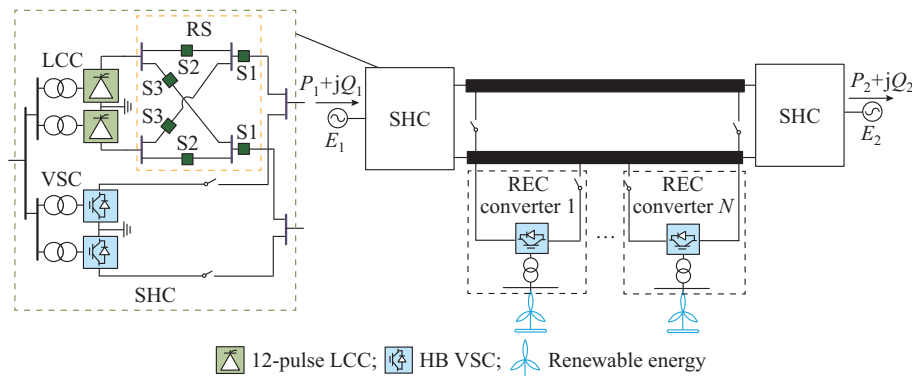


Fig. 2. Topology of proposed hybrid MTDC system.

B. Control of SHC in Hybrid MTDC System

The basic control of the SHC in the hybrid MTDC system is shown in Fig. 3, where v_L and v_v are the output voltages of LCC and VSC, respectively; i_v is the output current of VSC; u_v is the AC voltage of point of common coupling (PCC); R_L and R_v are resistances of the interfacing reactor; L_L and L_v are inductances of the interfacing reactor; $f_{ref,remote}$ and f_{remote} are the reference and measured remote frequencies, respectively; $f_{ref,local}$ and f_{local} are the reference and measured local frequencies, respectively; CC is constant current control; CEA is constant extinction angle control; CAPC is constant active power control; CDVC is constant DC voltage control; and CRPC is constant reactive power control.

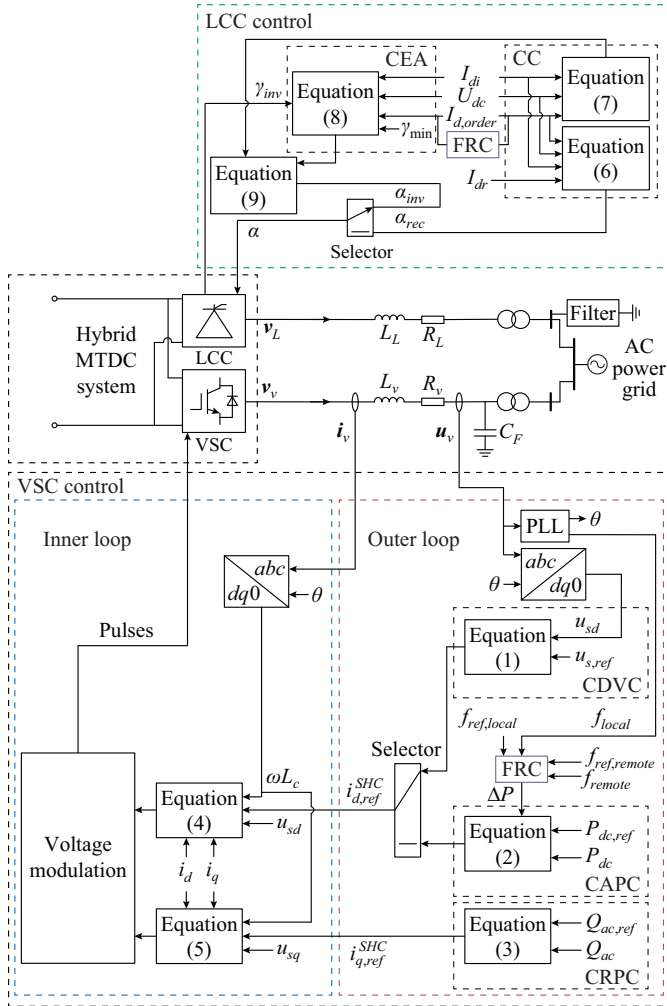


Fig. 3. Basic control of SHC.

The VSC control principle is given by (1)-(5), and the LCC control principle is given by (6)-(10).

1) VSC control:

$$i_{d,ref}^{SHC} = (u_{s,ref}(s) - u_{sd}(s)) \left(k_p^{dc} + \frac{k_i^{dc}}{s} \right) \quad (1)$$

$$i_{d,ref}^{SHC} = (P_{dc,ref}(s) - P_{dc}(s) + \Delta P) \left(k_p^p + \frac{k_i^p}{s} \right) \quad (2)$$

$$i_{q,ref}^{SHC} = (Q_{ac,ref}(s) - Q_{ac}(s)) \left(k_p^q + \frac{k_i^q}{s} \right) \quad (3)$$

$$u_{vd,ref}(s) = u_{sd}(s) - \omega L_c i_q(s) + (i_{d,ref}^{SHC}(s) - i_d(s)) \left(k_p^{ud} + \frac{k_i^{ud}}{s} \right) \quad (4)$$

$$u_{vq,ref}(s) = u_{sq}(s) - \omega L_c i_d(s) + (i_{q,ref}^{SHC}(s) - i_q(s)) \left(k_p^{uq} + \frac{k_i^{uq}}{s} \right) \quad (5)$$

where $i_{d,ref}^{SHC}$ and $i_{q,ref}^{SHC}$ are the reference values of d - and q -axis currents for SHC, respectively; $u_{s,ref}$ and u_{sd} are the reference and measured values of DC voltage, respectively; $P_{dc,ref}$ and P_{dc} are the reference and measured values of active power, respectively; ΔP is the power order generated from FRC; $Q_{ac,ref}$ and Q_{ac} are the reference and measured values of reactive power, respectively; $u_{vd,ref}$ and $u_{vq,ref}$ are the d - and q -axis reference voltages on the converter side, respectively; u_{sd} and u_{sq} are the d - and q -axis voltages on the AC system side, respectively; ω is the AC system angular frequency; L_c is the equivalent reactance of AC system; i_d and i_q are the d - and q -axis currents for SHC, respectively; k_p^{dc} and k_i^{dc} are the proportional and integral gains of DC voltage controller, respectively; k_p^p and k_i^p are the proportional and integral gains of active power controller, respectively; k_p^q and k_i^q are the proportional and integral gains of reactive power controller, respectively; k_p^{ud} and k_i^{ud} are the proportional and integral gains of d -axis current controller, respectively; and k_p^{uq} and k_i^{uq} are the proportional and integral gains of q -axis current controller, respectively.

2) LCC control:

$$\alpha_{rec} = \pi - (I_{dr} - \min\{VDCOL(U_{dc} + 0.01I_{di}), I_{d,order}\}) \left(k_p^{rec} + \frac{k_i^{rec}}{s} \right) \quad (6)$$

$$\beta_{inv,CC} = (\min\{VDCOL(U_{dc} + 0.01I_{di}), I_{d,order}\} - I_{di} - 0.1) \left(k_p^{CC} + \frac{k_i^{CC}}{s} \right) \quad (7)$$

$$\begin{cases} \beta_{inv,CEA} = \max\{UI_{inv}, -0.544\} \left(k_p^{CEA} + \frac{k_i^{CEA}}{s} \right) \\ UI_{inv} = CBC((\min\{VDCOL(U_{dc} + 0.01I_{di}), I_{d,order}\} - I_{di}) + \gamma_{min} - \gamma_{inv}) \end{cases} \quad (8)$$

$$\alpha_{inv} = \pi - \max\{\beta_{inv,CC}, \beta_{inv,CEA}\} \quad (9)$$

where α_{rec} is the firing angle of the LCC rectifier; α_{inv} is the firing angle of the LCC inverter; $\beta_{inv,CC}$ is the firing advanced angle of the LCC inverter with CC control; $\beta_{inv,CEA}$ is the firing advanced angle of the LCC inverter with CEA control; U_{dc} is the DC voltage for LCC; I_{dr} is the DC current of LCC rectifier; I_{di} is the DC current of LCC inverter; γ_{inv} is the extinction angle of LCC inverter; γ_{min} is the minimum extinction angle of LCC inverter; k_p^{rec} and k_i^{rec} are the proportional and integral gains of current controller for LCC rectifier, respectively; k_p^{CC} and k_i^{CC} are the proportional and integral gains of current controller for LCC inverter, respectively; k_p^{CEA} and k_i^{CEA} are the proportional and integral gains of extinction angle controller for LCC inverter, respectively; $I_{d,order}$ is the DC current reference of the LCC; $CBC(\cdot)$ is the function for DC current bias control (CBC); and the voltage

dependent current order limiter (VDCOL) is given by:

$$I = \begin{cases} 0.55 & U \leq 0.4 \\ 0.9U + 0.19 & 0.4 < U \leq 0.9 \\ U + 0.1 & U > 0.9 \end{cases} \quad (10)$$

C. Control Structure of REC Converter in Hybrid MTDC System

Owing to the difference in the put-into-operation time of the renewable energies, the connection configurations for integration of renewable energies into the hybrid MTDC system could be sorted into two configurations: direct connection to the hybrid MTDC system and double connection to AC+hybrid MTDC system, as shown in Fig. 4.

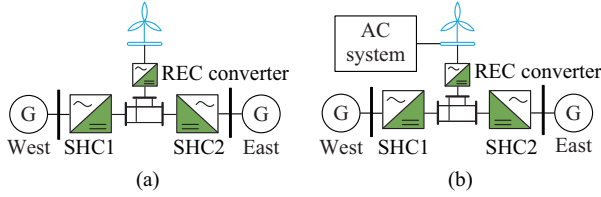


Fig. 4. Connection configurations for integration of renewable energies into hybrid MTDC system. (a) Direct connection. (b) Double connection to AC+hybrid MTDC system.

1) REC Control (Direct Connection)

The application scenario of renewable energies direct connection to the hybrid MTDC system with the REC converters mainly includes the newly-installed renewable energies such as offshore wind farm, which are usually in a passive network. In this configuration, the REC converters work at constant FRC and constant AC voltage control to provide stable frequency and AC voltage references for wind turbine (WTs). The basic control logic of REC converter in direct connection configuration is shown in Fig. 5, where ω_0 is the nominal grid frequency; v_w is the wind speed; i_r and i_g are the currents of rotor-side converter (RSC) and grid-side converter (GSC), respectively; and i_w is the current from WT.

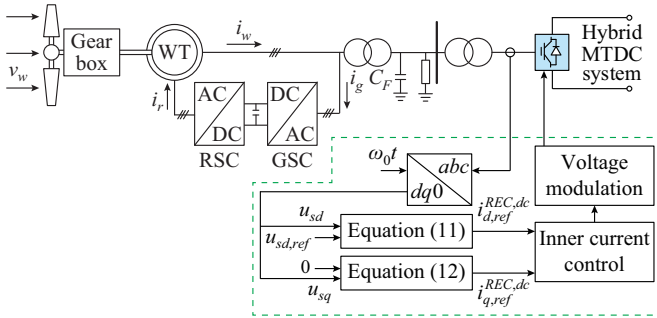


Fig. 5. Basic control logic of REC converter in direct connection configuration.

The control principle for REC converter in direct connection configuration is given by (11) and (12).

$$i_{d,ref}^{REC,dc} = (u_{sd,ref}(s) - u_{sd}(s)) \left(k_p^{ud} + \frac{k_i^{ud}}{s} \right) \quad (11)$$

$$i_{q,ref}^{REC,dc} = (0 - u_{sq}(s)) \left(k_p^{uq} + \frac{k_i^{uq}}{s} \right) \quad (12)$$

where $i_{d,ref}^{REC,dc}$ and $i_{q,ref}^{REC,dc}$ are the reference values of d - and q -axis currents for REC converter in direct connection configuration, respectively.

2) REC Control (Double Connection to AC+Hybrid MTDC System)

For the operating renewable energy projects, adopting the direct connection configuration to replace the existed AC connection is wasteful and unpractical. Considering the flexibility of the hybrid MTDC system, in this paper, the double connection configuration to AC+hybrid MTDC system is proposed for the existing renewable energy project to improve their controllability and stability. In this configuration, the renewable energy projects connect to the hybrid MTDC system via a DC intertie while keeping the connection to the AC system. This configuration could significantly optimize the power flow distribution of the renewable energies, thereby reducing the potential power congestion in their connected AC system and improving the operating economy.

Different from the direct connection configuration for the integration of renewable energies, in the double connection configuration, the REC converter could work at CAPC to realize the accuracy control of power injection to the hybrid MTDC system. In addition, the REC converter in the double connection configuration needs to have the ability to provide frequency and AC voltage references under the AC connection outage, for guaranteeing the operation stability of the renewable energy generations under the contingencies. Considering the control requirements of the REC converter in the double connection configuration, the power synchronization loop (PSL) is implemented for the REC converter control. The basic control logic of the REC converter in double connection configuration is shown in Fig. 6.

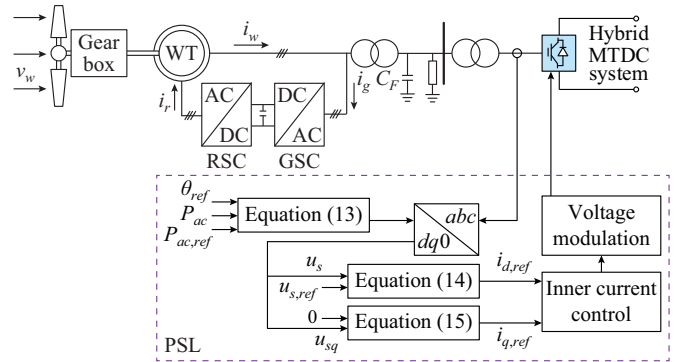


Fig. 6. Basic control logic of REC converter in double connection configuration.

As shown in Fig. 6, different from traditional phase lock loop (PLL), the PSL synchronizes the REC converter with the AC system by CAPC. The value of θ used in Park transformation of the converter could be expressed as (13). The control principle for REC converter in double connection configuration is given by (14) and (15).

$$\theta = \int (P_{ac,ref} - P_{ac}) \left(k_p^{PSL} + \frac{k_i^{PSL}}{s} \right) dt + \theta_{ref} \quad (13)$$

$$i_{d,ref}^{REC,dc} = (u_{s,ref}(s) - u_s(s)) \left(k_p^{ud} + \frac{k_i^{ud}}{s} \right) \quad (14)$$

$$i_{q,ref}^{REC.doc} = (0 - U_{sq}(s)) \left(k_p^{uq} + \frac{k_i^{uq}}{s} \right) \quad (15)$$

where $i_{d,ref}^{REC.doc}$ and $i_{q,ref}^{REC.doc}$ are the reference values of d - and q -axis currents for REC converter in double connection configuration, respectively; and $P_{ac,ref}$ and P_{ac} are the reference and measured active power on the PCC bus, respectively.

With the complete basic control structure, the hybrid MTDC system could integrate various types and operation modes of renewable energies. Moreover, the hybrid MTDC system could meet different requirements of the system operator for various operation conditions by the control coordination of multiple terminals. The system-level control strategies of the hybrid MTDC system are introduced in the following sections.

III. FLEXIBLE POWER FLOW CONTROL OF HYBRID MTDC SYSTEM

A. Operation Modes of Hybrid MTDC System

In the analysis of [7], the efficient utilization of renewable energies and the load diversity in the U.S. may contribute to the main financial benefit. The station-hybrid topology and corresponding control strategies proposed in [19] could realize uninterrupted power flow reversal, but due to the two-terminal structure, the renewable energies not near the pathway cannot achieve the integration. The proposed hybrid MTDC system provides an attractive solution for much higher integration rate of renewable energies in the U.S. power grid. Different from the proposed topology in [19], the hybrid MTDC system adopts new operation modes and control strategies to keep the flexible power flow characteristic while realizing the uninterrupted integration of renewable energies.

According to the potential operation conditions of the hybrid MTDC system for North America cross-seam interconnection, its operation modes could be summarized as Fig. 7, wherein, as an example illustration, a wind farm is integrated into the hybrid MTDC system through an intermediate terminal, where P_{LCC1} , P_{VSC1} , P_{LCC2} , P_{VSC2} , and P_{REC} are the ideal power flows on the LCC1, VSC1, LCC2, VSC2, and REC converters, respectively.

In the steady state, if the power reference is set smaller than the capacity of LCCs, the power on the hybrid MTDC system only flows through the LCCs. If the power reference is set larger than the capacity of LCCs, the VSCs transmit the rest power of the power reference. This transmission strategy could reduce the transmission loss. Moreover, the VSCs could keep the capacity for supporting emergency operation conditions.

During the operation mode conversion, the hybrid MTDC system must keep the system operation because the integration of renewable energies cannot be terminated.

B. Flexible Power Flow Control of Hybrid MTDC System

For satisfying the flexible and uninterrupted integration of renewable energies, a flexible power flow control is proposed in this paper. The flexible power flow control strategies with the example power flow direction changes between SHC1 and SHC2 are shown in Table I and Fig. 8.

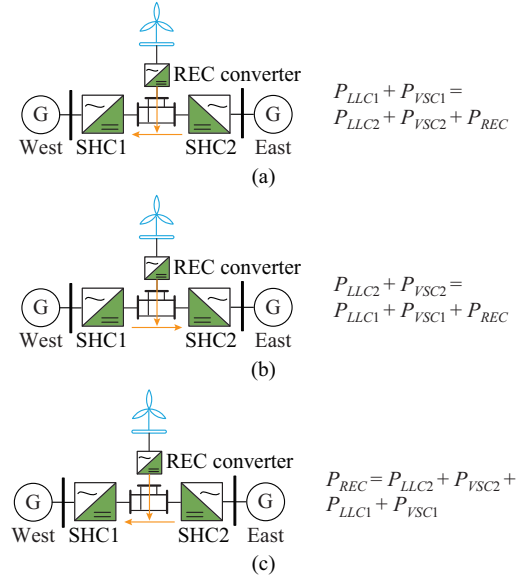


Fig. 7. Operation modes of hybrid MTDC system. (a) East to West. (b) West to East. (c) Renewable energies to both sides.

TABLE I
FLEXIBLE POWER FLOW CONTROL STRATEGIES

Control step	Control scheme
Initial condition	LCC1: CC; LCC2: CEA; VSC1: CPAC; VSC2: CAPC
Step I	<ol style="list-style-type: none"> 1) Decrease the active power of LCC1 to the minimum value with a constant ramping rate, then block LCC1. 2) Disconnect LCC1 from the system by opening S1 (RS_b).
Step II	<ol style="list-style-type: none"> 1) Reverse voltage polarity of LCC1 by opening S2 and closing S3 (RS_d). 2) Reconnect LCC1 to the system by closing S1 (RS_a), unblock LCC1. 3) LCC2 changes to CC while VSC2 changes to CDVC. 4) Decrease the active power of LCC2 while increase the active power of LCC1 with the same ramping rate until the power flow through LCC2 to its minimum value, then block LCC2. 5) Disconnect LCC2 from the system by opening S1 (RS_b) and reverse voltage polarity of LCC2 by opening S2 and closing S3 (RS_d).
Step III	<ol style="list-style-type: none"> 1) Increase the active power of LCC1, meantime, reverse and increase the active power of VSC1 to fully integrate renewable energies. 2) Reconnect LCC2 to the system by closing S1 (RS_a). 3) Unblock LCC2 and increase the active power of LCC2. 4) LCC2 changes to CEA while VSC2 changes to CAPC.

In Fig. 8, the initial power flow of the hybrid MTDC system is assumed from West (SHC1) to East (SHC2). The RS mechanism adopted for the voltage polarity reverse is shown in Fig. 9, which is referred to our previous work [19].

As shown in Table I, the flexible power flow control strategy is comprised of three steps. Utilizing the proposed flexible power flow control, the hybrid MTDC system can coordinate the power flow between the SHCs and RECs, thereby reversing the power flow while keeping the uninterrupted system operation.

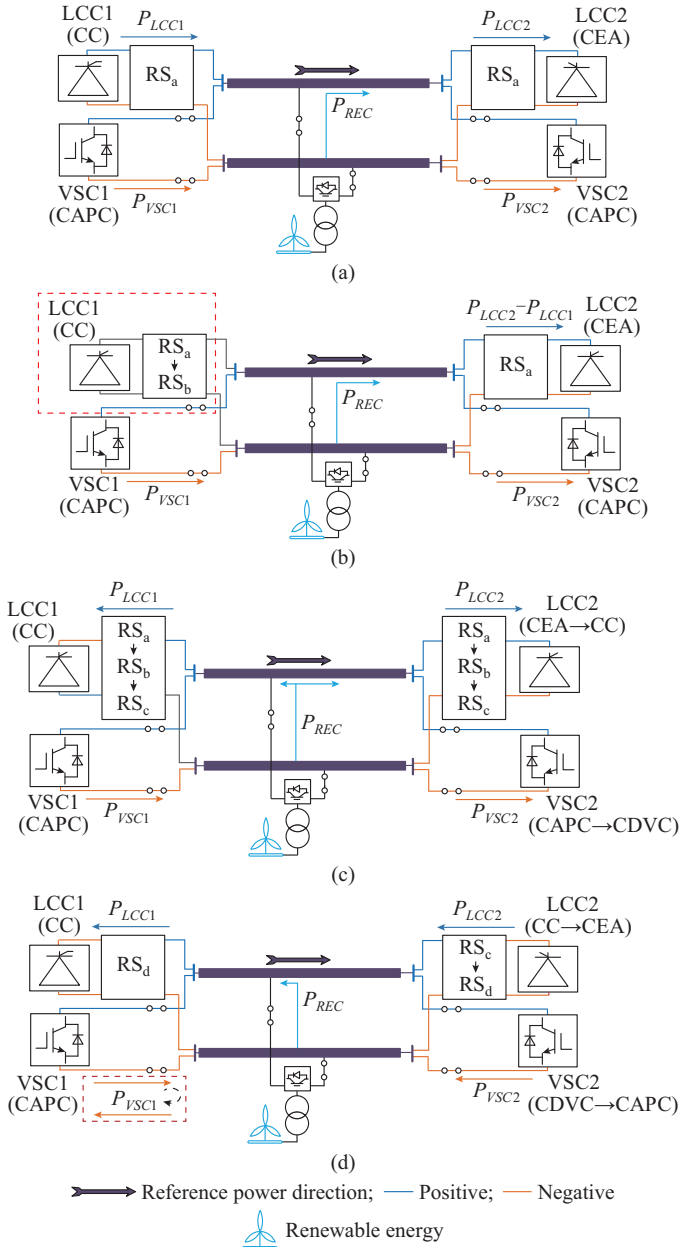


Fig. 8. Flexible power flow control strategies with example power flow direction changes between SHC1 and SHC2. (a) Initial condition. (b) Step I. (c) Step II. (d) Step III.

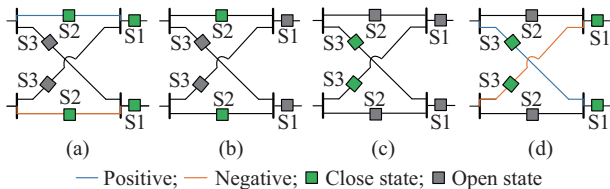


Fig. 9. Operation conditions of RS mechanism. (a) RS_a . (b) RS_b . (c) RS_c . (d) RS_d .

Moreover, owing to that the integrating capacity of the renewable energies is smaller than the SHC capacity, during the power flow reversal process, the power flow injection of renewable energies is the same as normal operation conditions. Therefore, different from the topology and corresponding control strategies [19], the proposed hybrid MTDC sys-

tem achieves the bulk power flow optimization between the interconnections while guaranteeing the uninterrupted and large-scale integration of renewable energies during the power flow reversal.

IV. FREQUENCY RESPONSE OF HYBRID MTDC SYSTEM

A. Frequency Service Sharing Between Interconnections

The reliability service sharing between the interconnections brings diversity to the service choosing, which benefits both interconnections and their market participators. Owing to the excellent controllability and flexible operation modes, the proposed hybrid MTDC system could provide multiple reliability services, which achieves the adequate employment of the system and creates additional values. Sharing frequency response reserves through the MTDC system is expected to provide large potential benefits to its connected interconnections. Each interconnection could rely, in part, on the spinning reserves, inertia, and governor response of the neighboring interconnection to provide FRS during an event through the proposed hybrid MTDC system. Recent DOE study has also proved that the frequency response sharing could provide 25% of the economic benefits, which is the second large part of the economic benefit behind load diversity [7]. In this paper, FRC is developed on the proposed hybrid MTDC system.

B. FRC of Hybrid MTDC System

The advantage of the LCC is that it could provide overload capacity support. According to the practical experience, the long-term overload capacity of the LCC is designed with 10%-20% capacity and the transient overload capacity of LCC could be up to 40%-50% capacity [23]. Compared with the LCC, the VSC could realize the fast power flow reversal and reactive power support. The hybrid MTDC system could combine both advantages of LCC and VSC at frequency responses, thereby providing better frequency regulation service to the interconnections while keeping enough capacity for enhancing the system security against the next contingency. The control strategy of proposed FRC is depicted in (16)-(20) and Fig. 10, where k_p^{fre} and k_p^{flc} are the droop coefficients; and ASC is short for ancillary service control.

$$-P_{VSC,limit} \leq P_{VSC} + \Delta P_f \leq P_{VSC,limit} \quad (16)$$

$$\begin{cases} \Delta P_1 = \Delta P_f - P_{VSC,limit} \\ \Delta P_2 = P_{VSC,limit} - P_{VSC} \end{cases} \quad (17)$$

$$-P_{SHC} \leq P_{VSC} + \Delta P_f \leq P_{SHC} \quad (18)$$

$$-P_{LCC,limit} \leq P_{LCC} + \Delta P_f \leq P_{LCC,limit} \quad (19)$$

$$\begin{cases} \Delta P_3 = P_{LCC,limit} - P_{LCC} \\ \Delta P_4 = \Delta P_f - P_{LCC,limit} \end{cases} \quad (20)$$

As shown in Fig. 10, the FRC continuously monitors the frequency and converts the frequency oscillation to power order deviation ΔP_f . If the ΔP_f is under the transfer limit of VSC $P_{VSC,limit}$, the frequency oscillation is only regulated by VSC until the frequency is stabilized. Then, the supported power will be reallocated from VSC to LCC for reducing the

transmission loss ($LCC_{loss} < VSC_{loss}$) while keeping the regulating capacity of VSC. If the increase of ΔP_f is over $P_{VSC,limit}$ and the frequency is not stable, the newly increasing support power will be regulated by LCC. If ΔP_f is over the total capacity of SHC, the LCC can increase output over its capacity $P_{LCC,limit}$ in a short time to provide emergency power support.

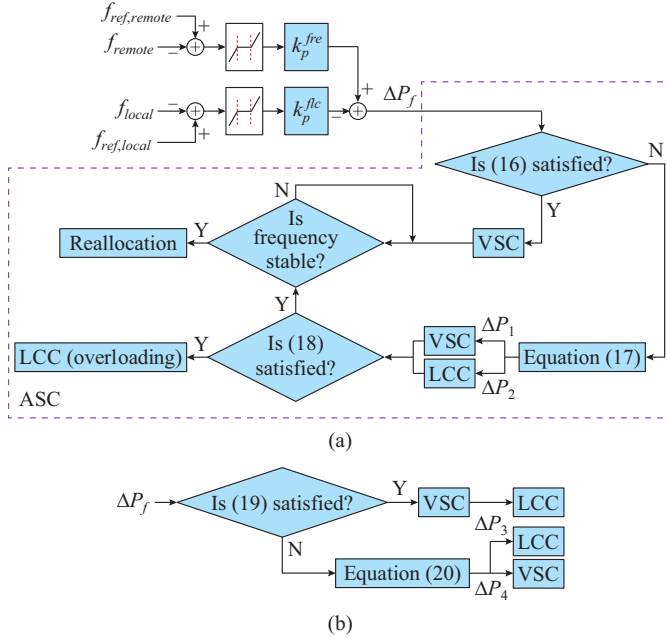


Fig. 10. Control strategy of FRC. (a) Control strategy. (b) Reallocation.

Different from the traditional HVDC transmission system, the FRC makes full use of the advantages of a hybrid MTDC system. The regulating range of the hybrid MTDC system at frequency response is enlarged through the overloading capacity of LCC. In addition, the supported power reallocation could reduce the transmission loss after the event, meantime, realizing the fast recovery of the emergency regulating capacity of the VSC can increase the resilience of the hybrid MTDC system to enhance the security against the continuous faults.

V. CASE STUDY OF HYBRID MTDC SYSTEM

In this section, a hybrid MTDC test system, as depicted in Fig. 3, is implemented in PSCAD/EMTDC to validate the performance of the proposed hybrid MTDC system. In the test system, two REC converters are considered. The system parameters of the LCC are the same as the CIGRE benchmark standard model parameters [24]. The system parameters of the VSC are the same as [25]. The basic parameters of the test hybrid MTDC system are shown in Table II. The wind farm that REC converter connects to is comprised of 150 doubly-fed inductive generators (DFIGs), and the capacity of each DFIG is 5 MW. The parameters of the DFIGs are shown in Table III. The droop coefficient of FRC is 14000 MW/Hz. The AC system adopted in this paper is the equivalent single-machine model, the inertia constant H and the short-circuit ratio SCR are 18.11 s and 10, respectively.

TABLE II
PARAMETERS OF HYBRID MTDC SYSTEM

Converter	Rated AC voltage (kV)	Rated DC voltage (kV)	Rated DC current (kA)	Rated power (MW)	DC line length (km)
SHCs	LCC1&LCC2	500	±500	3000	1000
	VSC1&VSC2	500	±500	1000	1000
REC converter	500	±500	0.75	750	1000

TABLE III
PARAMETERS OF DFIG

Parameter	Value
Rated voltage (kV)	0.69
Rated apparent power (MVA)	5.556
Rated mechanical power (MW)	4.870
Number of pole pairs	2
Nominal speed (rad/min)	1485.153
Stator resistance (p.u.)	0.01
Stator reactance (p.u.)	0.1
Magnetizing reactance (p.u.)	3.5
Rotor resistance (p.u.)	0.056
Rotor reactance (p.u.)	0.031

In the initial state, the LCC1 works at CC, the LCC2 works at CEA, and the VSC1 and VSC2 work at CAPC. The reference DC voltage of LCC2 is set as 460 kV in order to keep the DC voltage of the LCC1 at 500 kV (1 p.u.).

A. Case 1: Uninterrupted Integration of Renewable Energies

The test scenario for the interrupted integration of renewable energies is conducted to verify the integrating capacity of the hybrid MTDC system for renewable energies. In practice, the HVDC system power regulation under the normal operation is slow, which is up to 100 MW/min [26]. In order to shorten the simulation process, the power ramping rate is set as 1000 MW/s in this section. In this case, the REC1 adopts the direct connection configuration and the REC2 adopts the double connection configuration. The initial condition is as follows. Before $t=6$ s, the hybrid MTDC system transmits 1500 MW power from SHC1 to SHC2 and it is assumed that the connected renewable energies work at the rated power and the REC2 transmits 400 MW power from SHC1 to SHC2. At $t=6$ s, the AC connection of the renewable energies occurs an outage. The REC2 changes to PSL control.

Figure 11 depicts the performance of hybrid MTDC system for the uninterrupted integration of renewable energies. Before $t=6$ s, as shown in Fig. 11(e), the REC1 absorbs all the power generated from its connected renewable energies

to the hybrid MTDC system and the REC2 transmits the fixed power (400 MW) to the hybrid MTDC system. With the integration of renewable energies, the DC voltage of the hybrid MTDC system and the AC voltages of PCC with REC converters remain stable. The injected power from renewable energies via REC converters are transmitted to SHC2. At $t=6$ s, due to the outage at AC connection of renewable energies, the REC2 changes to PSL control. As shown in Fig. 11(e), in order to stabilize the frequency and AC voltage of the renewable energies, the REC2 changes its operation mode from a fixed power injection (400 MW in this case) to absorb all the power generated from renewable energies. The power injection from REC2 to hybrid MTDC system is changed from 400 MW to 750 MW. Due to the flexible control of the hybrid MTDC system, the LCC2 in

the SHC2 absorbs all the increased power from REC2. As shown in Fig. 11(d), the power flow through SHC2 is changed from 2650 MW to 2810 MW and stabilizes at 2680 MW. During the outage event at AC connection, as shown in Fig. 11(a) and (b), the AC voltage and frequency of the PCC with REC2 have a small oscillation then are stabilized at an acceptable level. In addition, as shown in Fig. 11(c) and (f), the power flow through SHC1 is stable, and the power output of renewable energies has a small oscillation but its operation safety is not influenced. The simulation results indicate that the hybrid MTDC system could achieve the flexible and uninterrupted integration of renewable energies and could provide multiple connection support for the different operation requirements of renewable energies.

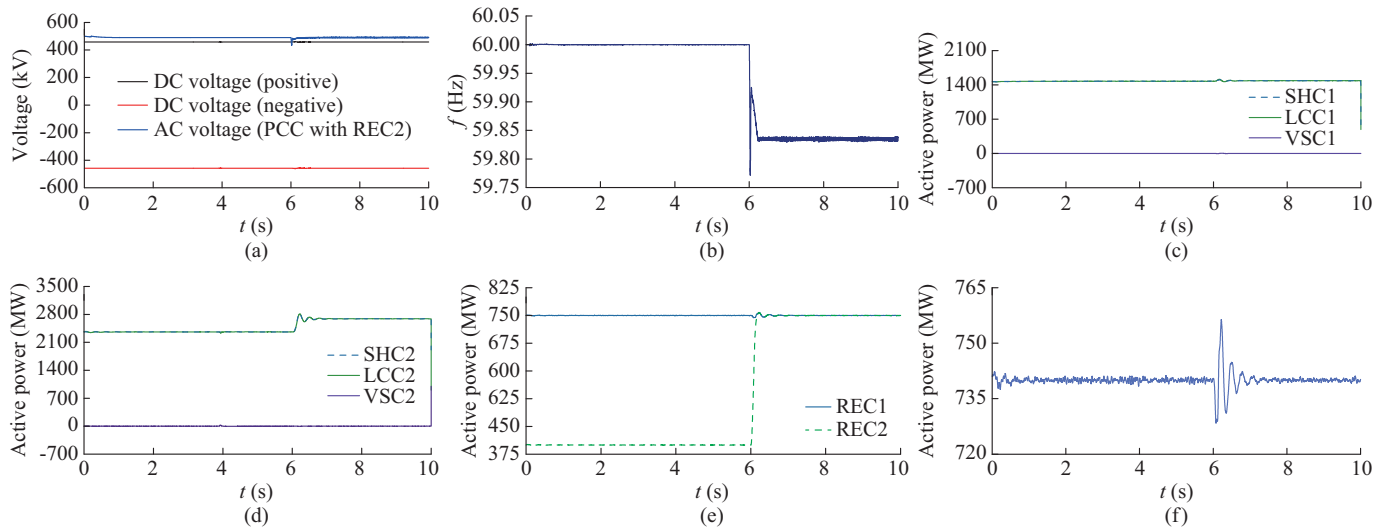


Fig. 11. Performance of hybrid MTDC system in case 1. (a) Voltage. (b) Frequency of PCC with REC2. (c) Active power through SHC1. (d) Active power through SHC2. (e) Active power of REC converters. (f) Active power of renewable energies.

B. Case 2: Flexible Power Flow Control

The test scenario for flexible power flow control is conducted to verify that the proposed flexible power flow control could achieve the bidirectional power flow control while realize the uninterrupted integration of renewable energies. In order to shorten the simulation process, the power ramping rate is set as 1000 MW/s, the same as case 1. In this case, the hybrid MTDC system transmits 2500 MW power from SHC1 to SHC2. The REC converters adopt the direct connection configuration for renewable energies. It is assumed that the connected renewable energies work at rated power and the REC converters transmit 1500 MW power to SHC2. The operation sequence of the proposed flexible power flow control of the hybrid MTDC system is as follows.

1) $t=0.5$ s- 3.5 s, the LCC1 decreases from 2500 MW to the minimum value with a constant ramping rate, then the LCC1 is blocked.

2) $t=3.5$ s- 4.5 s, the LCC1 is disconnected from the MTDC system by the mechanical switch, then the voltage polarity of LCC1 is reversed via RS mechanism. After the voltage polarity reversal, the LCC1 is reconnected to the MTDC system.

3) $t=4.5$ s- 5.0 s, the LCC2 changes to CC and the power order adopts its operation power, and the VSC2 changes to CDVC to control the DC voltage. Then, LCC2 decreases to the minimum value while LCC1 is unblocked and increases with the same ramping rate until LCC2 is automatically blocked.

4) $t=5.0$ s- 6.0 s, the LCC2 is disconnected from the MTDC system by the mechanical switch, then the voltage polarity of LCC2 is reversed via RS mechanism. At the same time, the LCC1 further increases power until the power flow through the REC converters is transmitting to SHC1.

5) $t=6.0$ s- 9.5 s, the LCC2 is reconnected to the MTDC system with a mechanical switch. The LCC2 is unblocked and the LCC2 changes its operation mode to CEA. Meantime, the VSC2 also changes its operation mode to CDVC, and the power order adopts its operation power. Then the LCC1, VSC1, and VSC2 increase the active power to the power reference.

Figure 12 depicts the performance of the hybrid MTDC system during the power flow reversal process. As shown in the simulation results, the DC voltage is stable during the whole power flow reversal process. This indicates that all the converters (SHCs & REC converters) could keep the nor-

mal work condition during this period, and the DC voltage is under control. Besides, as shown in Fig. 12(b)-(d), during this period, there exists only a small fluctuation in the power rising and falling processes. This indicates that the hybrid MTDC system is still stable and meets the operation reliabili-

ty requirement. The simulation results indicate that, with the proposed flexible power flow control, the hybrid MTDC system could realize the bidirectional and uninterrupted power transmission without influencing the integration of renewable energies.

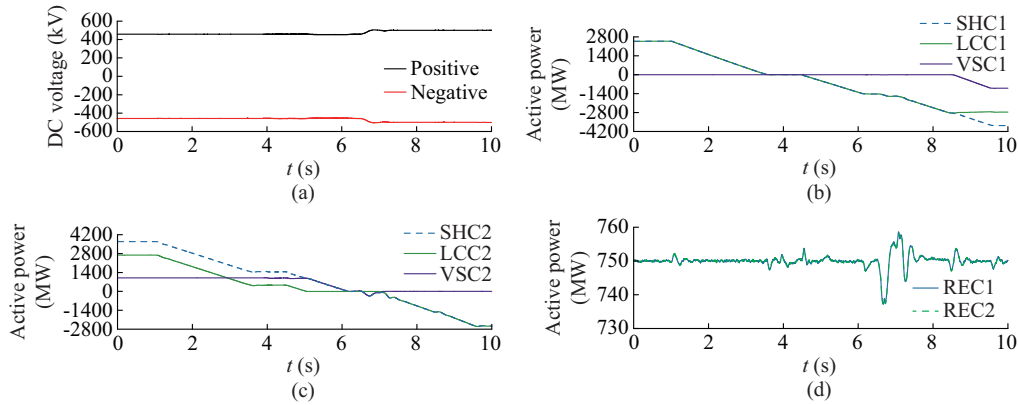


Fig. 12. Performance of hybrid MTDC system in case 2. (a) DC voltage. (b) Active power through SHC1. (c) Active power through SHC2. (d) Active power of REC converters.

C. Case 3: FRC

The test scenario for FRC is implemented to verify the regulating range and flexible controllability of the hybrid MTDC system under contingencies. The initial condition is as follows. Before $t=2$ s, the hybrid MTDC system transmits 2000 MW power from SHC1 to SHC2 and the output of renewable energy is 1500 MW. At $t=2$ s, a 1000 MW generator is tripped at East. In this case, the response of the generator in the interconnections is not considered. In practice, the power regulation of HVDC system under the event could be up to 200 MW/s [26]. In order to shorten the simulation process, the power ramping rate is set as 2000 MW/s. In this case, the RECs adopt the direct connection configuration for the renewable energies, and the REC converters transmits 1500 MW power to SHC2. The operation sequence of the proposed grid support control of the hybrid MTDC system is as follows.

1) $t=2.0$ s- 3.75 s, since the support power direction of the FRC is the same as the power flow direction of the hybrid MTDC system but the VSC2 has reached its maximum value 1000 MW, for meeting the support requirement, the VSC1 increases the power from 0 MW to 1000 MW (the maximum capacity). Although the power increase is over the capacity of LCC2, owing to the overloading capacity of LCC, the power flow through the LCC2 could be increased from 2200 MW to 3200 MW.

2) $t=6.0$ s- 7.0 s, when the frequency is stable, the reallocation control in FRC is activated. The VSC1 decreases its power from 1000 MW to 0 MW, and at the same time, the LCC1 increases its power from 2000 MW to 3000 MW. The ramping rates of the power increase of VSC and the power decrease of LCC are 1000 MW/s, which is the normal power regulation rate.

Figure 13 depicts the performance of hybrid MTDC system during the frequency response support process.

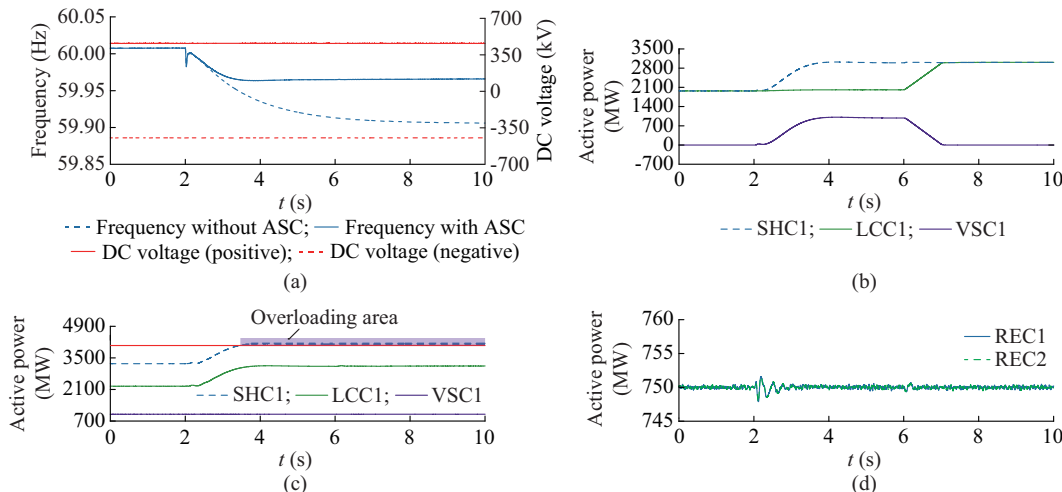


Fig. 13. Performance of hybrid MTDC system in case 3. (a) Frequency and DC voltage. (b) Active power through SHC1. (c) Active power through SHC2. (d) Active power of REC converters.

As shown in the simulation results, with the proposed FRC, the frequency nadir is significantly improved, which prevents the distributed system from working into an unacceptable condition. In addition, due to the LCC overloading capacity, the LCC2 could keep the 3200 MW until the generation of renewable energies reduces or the power flow dispatch is adjusted by the dispatching center. Moreover, the DC voltage of the hybrid MTDC system is still stable during the FRC process. It indicates that the frequency response support does not influence the normal operation of hybrid MTDC system. In addition, it could be seen from Fig. 13(b) and (c) that the FRC makes full use of the advantages of a hybrid MTDC system (LCC overloading capacity and power reallocation in SHC), which greatly enhances the reliability of interconnections.

VI. CONCLUSION

A hybrid MTDC transmission system is proposed in this paper for increasing the utilization and penetration of the national abundant renewable energies in the U. S. The main contributions of the paper are as follows.

1) Cost-effective bulk-power transmission

The capacity ratio between the LCC and VSC in the SHC is determined by system design requirements, and the rated capacity of LCC could be 2-3 times that of VSC. Therefore, the hybrid MTDC system could be cost-affordable for long-distance bulk power transmission system with intermediate converter stations for the integration of large-scale renewable energies.

2) Flexible delivery of large-scale renewable energies

The hybrid MTDC system could realize the flexible and interruptible power delivery of the interconnected renewable energies to SHC on either side or SHCs on both sides.

3) Flexible operation modes

With the co-existence of the LCC and VSC in both two SHCs, there is a flexible choice of operation modes of the proposed hybrid MTDC system. It could work as a full LCC system (blocking the VSCs in both two SHCs), full VSC system (blocking the LCCs in both two SHCs), terminal-hybrid system (blocking LCC in one SHC while blocking VSC in the other SHC), and pole-hybrid system (one pole only connected with LCCs and the other pole connected with VSCs).

4) Ancillary sharing between interconnections

The advantage of the LCC is that it could provide overcapacity support by its inherent overloading capacity, and the VSC could realize the fast power flow reversal and reactive power support. The hybrid MTDC system could combine both advantages of LCC and VSC at frequency responses, thereby providing a better frequency regulation service to the interconnections.

In future work, the DC fault ride-through capability of the proposed hybrid MTDC system, and the coordinated control of SHCs and renewable power plants connected to the hybrid MTDC system will be investigated.

REFERENCES

[1] IRENA. (2021, Apr.). North America renewable source. [Online]. Available: <https://www.irena.org/northamerica>

[2] C2ES. (2021, Apr.). Renewable energy. [Online]. Available: <https://www.c2es.org/content/renewable-energy/>

[3] K. Sun, K. Li, W. J. Lee *et al.*, "VSC-MTDC system integrating offshore wind farms based optimal distribution method for financial improvement on wind producers," *IEEE Transactions on Industry Applications*, vol. 55, no. 3, pp. 2232-2240, May-Jun. 2019.

[4] NREL. (2021, Apr.). Wind maps. [Online]. Available: <https://www.nrel.gov/gis/wind.html>

[5] NREL. (2021, Apr.). Solar maps. [Online]. Available: <https://www.nrel.gov/gis/solar.html>

[6] H. Zhao, Q. Wu, S. Hu *et al.*, "Review of energy storage system for wind power integration support," *Applied Energy*, vol. 137, pp. 545-553, Jan. 2015.

[7] NREL. (2021, Apr.). Interconnections seam study. [Online]. Available: <https://www.nrel.gov/analysis/seams.html>

[8] D. Jovicic and K. Ahmed. *High Voltage Direct Current Transmission: converters, Systems and DC grids*. New York: John Wiley & Sons, 2015.

[9] W. Yang, B. Zeng, and Y. Jia, "Simulation analysis of split connection mode system control for XiMeng to TaiZhou UHVDC project," in *Proceedings of 2018 International Conference on Power System Technology (POWERCON)*, Guangzhou, China, Nov. 2018, pp. 2972-2977.

[10] A. Egea-Alvarez, S. Fekriasl, F. Hassan *et al.*, "Advanced vector control for voltage source converters connected to weak grids," *IEEE Transactions on Power Systems*, vol. 30, no. 6, pp. 3072-3081, Nov. 2015.

[11] H. Xiao, Z. Xu, G. Tang *et al.*, "Complete mathematical model derivation for modular multilevel converter based on successive approximation approach," *IET Power Electronics*, vol. 8, no. 12, pp. 2396-2410, Dec. 2015.

[12] M. H. Nguyen, T. K. Saha, and M. Eghbal, "Master self-tuning VD-COL function for hybrid multi-terminal HVDC connecting renewable resources to a large power system," *IET Generation, Transmission & Distribution*, vol. 11, no. 13, pp. 3341-3349, Oct. 2017.

[13] H. Xiao, K. Sun, J. Pan *et al.*, "Review of hybrid HVDC Systems combining line communicated converter and voltage source converter," *International Journal of Electrical Power & Energy Systems*, vol. 129, pp. 106713, Jul. 2021.

[14] H. Xiao, K. Sun, J. Pan *et al.*, "Operation and control of hybrid HVDC system with LCC and full-bridge MMC connected in parallel," *IET Generation, Transmission & Distribution*, vol. 14, no. 7, pp. 1344-1352, Jan. 2020.

[15] HVDC News China. (2021, Apr.). Luxi hybrid BTB converter station. [Online]. Available: <https://hvdnewschina.blogspot.com/2017/09/luxi-hybrid-btb-converter-station.html>

[16] B. Qahraman, A. M. Gole, and I. Fernando, "Hybrid HVDC converters and their impact on power system dynamic performance," in *Proceedings of 2006 IEEE Power Engineering Society General Meeting*, Montreal, Canada, Oct. 2006, pp. 1-6.

[17] Z. Xu, S. Wang, and H. Xiao, "Hybrid high-voltage direct current topology with line commutated converter and modular multilevel converter in series connection suitable for bulk power overhead line transmission," *IET Power Electronics*, vol. 9, no. 12, pp. 2307-2317, Oct. 2016.

[18] X. Chen, H. Sun, J. Wen *et al.*, "Integrating wind farm to the grid using hybrid multiterminal HVDC technology," *IEEE Transactions on Industry Applications*, vol. 47, no. 2, pp. 965-972, Mar-Apr. 2011.

[19] K. Sun, H. Xiao, J. Pan *et al.*, "A station-hybrid HVDC system structure and control strategies for cross-seam power transmission," *IEEE Transactions on Power System*, vol. 36, no. 1, pp. 379-388, Jan. 2021.

[20] Y. Guo, H. Gao, and Q. Wu, "A combined reliability model of VSC-HVDC connected offshore wind farms considering wind speed correlation," *IEEE Transactions on Sustainable Energy*, vol. 8, no. 4, pp. 1637-1646, Oct. 2017.

[21] Y. Jiang-Häfner and Ludvika, "HVDC system and method to control a voltage source converter in a HVDC system," U. S. Patent 20090279328 A1, Nov. 12, 2009.

[22] W. Xiang, W. Lin, L. Xu *et al.*, "Enhanced independent pole control of hybrid MMC-HVDC system," *IEEE Transactions on Power Delivery*, vol. 33, no. 2, pp. 861-872, Apr. 2018.

[23] H. Rao, W. Wei, T. Miao *et al.*, "Frequency control at the power sending side for HVDC asynchronous interconnections between Yunnan power grid and the rest of CSG," *CSEE Journal of Power and Energy Systems*, vol. 7, no. 1, pp. 105-113, Jan. 2021.

[24] M. Szechtman, T. Wess, and C.V. Thio, "First benchmark model for HVDC control studies," *Electra*, vol. 135, pp. 54-73, Apr. 1991.

[25] M. Guan and Z. Xu, "Modeling and control of a modular multilevel

converter-based HVDC system under unbalanced grid conditions,” *IEEE Transactions on Power Electronics*, vol. 27, no. 12, pp. 4858-4867, Dec. 2012.

- [26] P. Belkin, “HVDC and power electronic systems for overhead line and insulated cable applications,” in *Proceedings of 2012 CIGRE San Francisco Colloquium*, San Francisco, USA, Mar. 2012, pp. 1-6.

Kaiqi Sun received the B.S. and Ph.D. degrees in electrical engineering from Shandong University, Jinan, China, in 2015 and 2020, respectively. He is currently a Research Associate in the Department of Electrical Engineering and Computer Science, The University of Tennessee, Knoxville, TN, USA. He is the recipient of the Best Student Paper Award from IEEE IAS I&CPS Asia, and the recipient of Excellent Paper Award from ECAI and SCEMS 2020. His research interests include control strategy of high-voltage direct current (HVDC) system and machine learning based power system application.

Huangqing Xiao received the B.S. and Ph.D. degrees in electrical engineering from Zhejiang University, Hangzhou, China, in 2013 and 2018, respectively. He is currently an Associate Professor in the School of Electric Power Engineering, South China University of Technology, Guangzhou, China. From 2018 to 2020, he was a Research Associate with the Department of Electrical Engineering and Computer Science, University of Tennessee, Knoxville, TN, USA. His research interests include high-voltage direct cur-

rent (HVDC) transmission, DC circuit breaker, and renewable power integration.

Jiuping Pan received the B.S. and M.S. degrees from Shandong University, Jinan, China, and the Ph.D. degree from Virginia Tech, Blacksburg, VA, USA. He is currently a Senior Principal Scientist with Hitachi-ABB Power Grids, Raleigh, NC, USA. His expertise and research interests include high-voltage direct current (HVDC) transmission and DC distribution systems and applications, power system planning and energy markets, and grid integration of large-scale renewable energies.

Yilu Liu received the M.S. and Ph.D. degrees from the Ohio State University, Columbus, USA, in 1986 and 1989, respectively. She received the B.S. degree from Xi’an Jiaotong University, Xi’an, China. Dr. Liu is currently the Governor’s Chair at the University of Tennessee (UJK), Knoxville, TN, USA and Oak Ridge National Laboratory (ORNL), Oak Ridge, TN, USA. Dr. Liu was elected as the member of National Academy of Engineering in 2016. She is also the Deputy Director of the Center for Ultra-Wide-Area Resilient Electric Energy Transmission Networks (CURENT). Prior to joining UTK/ORNL, she was a Professor at Virginia Tech. She led the effort to create the North American power grid frequency monitoring network (FNET) at Virginia Tech, which is now operated at UTK and ORNL as GridEye. Her current research interests include power system wide-area monitoring and control, large interconnection-level dynamic simulations, electromagnetic transient analysis, and power transformer modeling and diagnosis.